A&A 402, 361–372 (2003)
DOI: 10.1051/0004-6361:20030220

Astronomy & Astrophysics

On the nature of the chromospheric fine structure

I. Dynamics of dark mottles and grains

K. Tziotziou[1], G. Tsiropoula[1], and P. Mein[2]

[1] National Observatory of Athens, Institute for Space Applications and Remote Sensing, Lofos Koufos, 15236 Palea Penteli, Greece
e-mail: kostas@space.noa.gr; georgia@space.noa.gr
[2] Observatoire de Paris, Section de Meudon, LESIA, 92195 Meudon Principal Cedex, France
e-mail: pierre.mein@obspm.fr

Received 2 December 2002 / Accepted 24 January 2003

Abstract. We analyze a time series of forty high spatial and temporal resolution two-dimensional intensity and Doppler velocity images at different wavelengths within the Hα line. The observations were obtained with the Multichannel Subtractive Double Pass (MSDP) spectrograph at THEMIS. We study the morphology of dark mottles and grains as seen in different wavelengths and examine their relation to the MDI magnetic field topology. We determine some physical properties of dark mottles with an inversion technique based on an iterative cloud model method with constant source function, giving the optical thickness τ_0, the Doppler width $\Delta\lambda_D$, the velocity v and the source function S distribution along a structure. The obtained global properties of mottles as well as the spatial and temporal evolution of several physical parameters along the axes of individual mottles are discussed. The derived velocities in mottles as a function of space and time (time slice images) exhibit a quasi-periodic, bi-directional pattern. It is suggested that magnetic reconnection is the mechanism responsible for their formation and dynamics. Furthermore, a similar quasi-periodic behaviour of the Doppler velocity variations in dark grains and their morphological characteristics both suggest the similarity of dark mottles and grains.

Key words. Sun: chromosphere – lines: formation – radiative transfer

1. Introduction

The solar chromosphere, when seen in strong lines such as Ca II H and K and Hα is highly inhomogeneous. Outside active regions, the principal inhomogeneities are related to roughly cellular patterns, which constitute the "network". There is a clear distinction between the bright chromospheric patches, which make up the "network boundaries", and the somewhat darker areas, which constitute the "internetwork" (also called the "cell interiors"). It has also been shown that in the underlying photosphere, apart from sunspot and pores, the magnetic field is concentrated into small flux tubes with field strengths of 1–2 kG (Solanki 1993), which form patches of magnetic flux concentrations. A strong spatial coincidence exists between these magnetic flux concentrations and the overlying network boundaries. The network persists throughout the chromosphere-corona transition region and the low corona. Therefore, it is not surprising that several studies are devoted to better understand the network phenomena and the structures associated with it (see Rutten 1999 for a comprehensive review).

Send offprint requests to: K. Tziotziou,
e-mail: kostas@space.noa.gr

The chromospheric network is the locus of most of the quiet chromosphere fine structure and magnetic flux concentrations. This fine structure is different inside the network cells and its boundaries. In the cells many tiny, dark, round features are observed. Beckers (1968) observed them in the blue wing of Hα and called them grains. He also suggested that they may be identical to the bright grains observed in K_{2V} and K_3 lines, although their identity has not been firmly established. No further information is available about these structures at the level of the chromosphere. Several elongated bright and dark structures, (when seen in the Hα line), called mottles outline the network boundaries. Mottles seem to be very important features. They are considered as the disk counterparts of spicules and also as the principal channels through which mass and energy is supplied from the lower layers of the solar atmosphere to the corona and the solar wind.

Since the comprehensive review by Beckers (1972) and the monograph by Bray & Loughhead (1974) a lot of observational work has been performed aiming at shedding light on the physical properties of mottles and on their relation to spicules observed at the limb. On the basis of observational findings, various theoretical models have been developed to explain the mechanism responsible for their formation. However, in spite

of the remarkable advances made by the high-resolution observations within the last few years and by the development of theories, the diagnostics of their dynamics, the determination of several thermodynamic parameters, such as temperature and density, and the definition of a mechanism responsible for their formation are still uncertain. Ambiguities are due to the differences in their appearance when observed in different spectral lines, but also at different wavelengths within the same line, to the different methods used to infer physical parameters, especially velocities, and to their relatively short duration, small dimensions and rapid changes. There is, however, general agreement on some of their properties. Thus, it is now generally accepted that mottles are jet-like structures and that they cover, at any time, ∼1% of the solar surface. They have widths in the range 500–2000 km, reach heights in the range 5000–10 000 km above the photosphere and have lifetimes of 5–10 min. Their temperatures are believed to be of the order of 7000–15 000 K, their electron densities of the order of 4×10^{10}–10^{11} cm^{-3} and their gas pressures of the order of 0.2 dyn cm^{-2}. Indirect evidence based on similarities in dimension, lifetime, and physical conditions points to the identity of spicules and dark mottles (Tsiropoula & Schmieder 1997). It is also well-known that the arrangement of mottles is governed by the configuration of the local magnetic field. Thus mottles are usually organised into small groups, called chains and larger groups, called rosettes. In a chain the mottles point in the same direction. Rosettes have a circular shape and owe their morphology to the presence of magnetic canopy-like flux tubes filled by the plasma ejected from below and streaming outwards from a common bright center. Strong magnetic flux of the order of $\sim 10^{20}$ Mx has been detected in the bright center of a rosette, which is comparable to that of a pore (Dara-Papamargaritis & Koutchmy 1983).

Among other physical conditions, the study of the flows along these structures seen at the limb or on the disk is essential because it can add to the understanding of the mechanism driving them. Beckers (1963) reported that dark mottles, after disappearing in the Hα−0.5 Å image, often became visible in the Hα+0.5 Å, consistent with upflows followed by downflows. Suematsu et al. (1995) studied the apparent motions of mottles in Doppler images produced by red-blue wing subtraction and found that the great majority of them go up and then back down. Tsiropoula et al. (1994), using Beckers' cloud model (Beckers 1964), showed that the predominant pattern of bulk motion in dark mottles is that of downflows at their footpoints and alternating upflows and downflows at their tops. For structures seen at the limb, i.e. spicules, different and sometimes contradictory results on the velocity and its variations have been reported because of the different kind of observations. Thus, velocities have been inferred from studies of apparent motions, i.e. motions in the plane perpendicular to the line-of-sight, and from studies of Doppler shifts derived from spectroscopic observations, which yield the velocity component along the line-of-sight. In an old work Lippincott (1957), after studying the apparent motions of spicules, reported that the ascending phase is followed by a descending one; she was also the first to report that some spicules appear to rise from the same source several times. Reported time variations of Doppler shifts are also contradictory. Mouradian (1965) suggested that the velocity of spicules does not change sign, being always upwards; Pasachoff et al. (1968) found that Doppler velocities of a certain number of spicules do undergo quasi-periodic reversals. Recently, Wilhelm (2000), in a study of spicules observed in several EUV lines by SUMER on SOHO, reported strong red and blue shifts within a feature, which, furthermore, reverse sign. Although the connection between spicules seen in Hα and in EUV lines has not yet been firmly established, it is suggested that the EUV emission originates in a thin transition sheath separating the cool Hα-emitting spicular material from the hotter surrounding corona (Withbroe 1983). It is clear from the above that the behaviour of the flow along mottles and spicules remains an open question. There is, however, a strong observational support of the idea that the material along spicules shows alternating upward and downward motions.

A variety of mechanisms for generating mottles and spicules have been proposed. Roughly, these models can be put into four categories: models that are based on fluid instability, on hydrodynamic waves or rebound shocks, on Alfvén waves, and those based on reconnection of the magnetic field lines (see Sterling 2000 for a review). At present there is no clear choice as to the best model. Among these models, magnetic reconnection continues to be an attractive mechanism. Pikel'ner (1969) and Uchida (1969) proposed a similar model according to which spicules are generated from the interaction of opposite polarity magnetic field lines forced together by convective motions. This leads to reconnection of field lines and to the upward and downward motion of the material due to their reclosure. Tsiropoula et al. (1994) provided observational evidence of bi-directional flows in mottles followed by downflows and claimed that this flow pattern is consistent with the one expected to occur in the process of magnetic reconnection in accordance with the reconnection model proposed by Pikel'ner (1969). Recently, Wilhelm (2000) reported observations clearly showing the bi-directional character of the flows along spicules observed at the EUV and proposed magnetic reconnection as the driving mechanism of these structures.

The aim of this work is to use a long time series of high spatial and temporal resolution Hα spectro-images of the Sun to study some morphological properties of the dark chromospheric mottles and grains, to establish some of their physical properties and dynamical characteristics, to explore their association with the local magnetic field topology and to identify the driving mechanism responsible for their formation.

2. Observations

2.1. Observations and data reduction

A region containing a filament (S27 W05) was observed on May 14th, 2000 with the Multichannel Subtractive Double Pass (MSDP) spectrograph mounted on the French-Italian solar telescope THEMIS in Tenerife, Canary Islands. The MSDP spectrograph (Mein 1991, 2002) is designed to record a 2D field of view at several wavelengths within the line profile. Thus at each pixel of the image the line profile can be reconstructed. A large region of the solar surface can be quickly covered in several

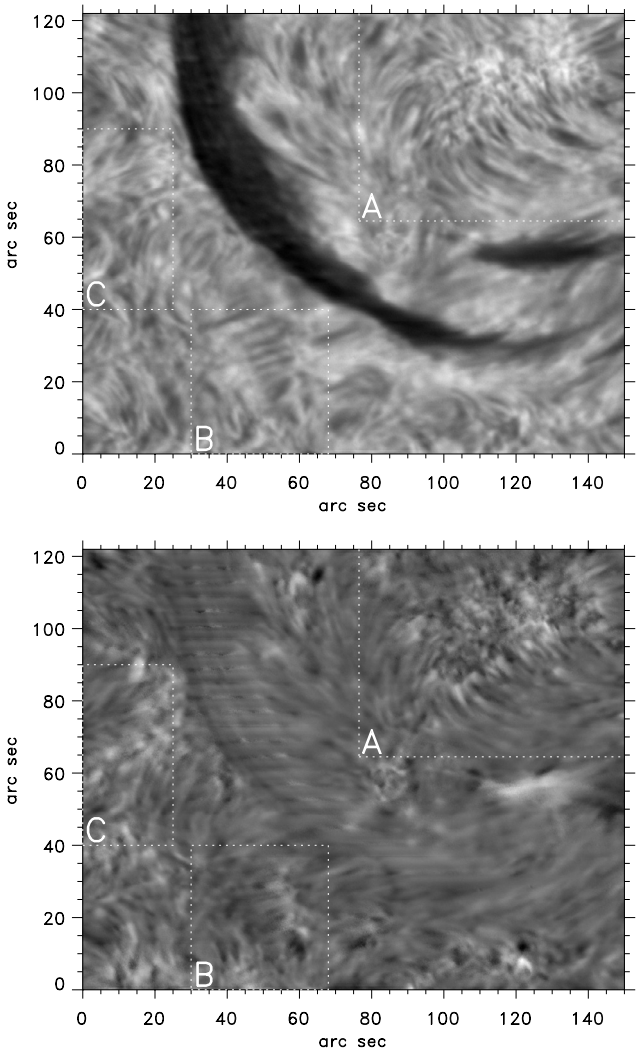

Fig. 1. Top panel: an intensity image of the observed region at +0.24 Å from the Hα line center. Bottom panel: a Doppler velocity image at ±0.24 Å (black corresponds to negative upward velocities). The dotted rectangular areas, denoted as A, B and C mark the three regions where mottles are mostly concentrated (see text).

wavelengths by displacing the entrance field stop of the telescope. The present time sequence of observations was obtained in the Hα line from 10:07 to 11:02 UT. During the observational sequence, eleven consecutive elementary images with a small overlap were recorded on a CCD camera every ~40.5 s in nine wavelengths, 0.24 Å apart, in the Hα profile. These were later combined with two-dimensional techniques of the MSDP reduction data package to form a single 150″ × 120″ large image (see Fig. 1) with a spatial resolution of about 0.5″. Eighty such images were finally reconstructed. However, because of distortion due to seeing only the first forty high resolution images of the time series were used for the present study. After correcting for flat field and dark current, using the aforementioned MSDP reduction package, intensity images at line center, ±0.24 Å and ±0.48 Å and Doppler velocity images at ±0.24 Å and ±0.48 Å have been obtained. The latter were derived using the bisector technique with the mean profile over the field-of-view (avoiding the brightest and darkest regions) as the reference profile.

2.2. Description of observations

In Fig. 1 a two-dimensional intensity map (upper panel) and Doppler velocity map (lower panel) of the entire field-of-view is presented. The direction of the solar north is towards top left and makes an angle of 21.°1 with the topward vertical of the image. Solar west is at right angles and points towards the right of the image. A filament consisting of several threads lies in a large channel and traverses diagonally the image. On both sides of the filament a large number of dark mottles can be identified in the intensity and Doppler velocity maps of Fig. 1. They are mostly concentrated in three regions, A, B and C (enclosed in boxes in Fig. 1) and form chains or rosettes (Bray & Loughhead 1974). Below we present a detailed description of the intensity and velocity maps in these regions as well as of the corresponding MDI magnetograms.

2.2.1. Intensity maps

Figure 2 shows a time sequence of region A at Hα line center, at +0.48 Å and −0.48 Å from the line center and the Doppler velocity at ±0.48 Å. This region, found at the upper right part of the image shown in Fig. 1, consists of several dark mottles forming a large rosette. Although part of it is found outside the upper and right part of the field-of-view it seems, from the MDI image of the region (Fig. 4), that it has an almost round shape with a radius of about 50 000 km. The central region of the rosette appears bright and contains several small round-shaped dark structures which are clearly visible in all images of Fig. 2. They have a typical radius of 1.5″–2″ and appear to be structures more or less vertical on the solar surface. These are the structures called “grains” by Beckers (1968). Around the central region of the rosette a large number of dark mottles is found. They are rooted at the boundaries of the central region and are extending outwards. The inner mottles are almost radially oriented with respect to the rosette center and have a lesser extent than the outer ones, which, furthermore, are not radial but are diverging counter-clockwise and run almost parallel to the two nearby filaments affected by their horizontal magnetic fields. The dark mottles of the rosette have a typical apparent thickness of ~2″ and lengths ranging from 10″ to 15″. They do not reach the center of the rosette and appear to be brighter at their footpoints. The rosette is not deformed during the whole one hour duration of our Hα observations. However, individual mottles undergo substantial changes in shape, direction and length. Although the large number of mottles around the rosette makes identification quite difficult, most of them can be followed from frame to frame. At Hα+0.48 Å and Hα–0.48 Å dark mottles become finer and more distinct than at line center. Comparison of images on these opposite wings shows differences in the size of the mottles due to the different contrasts. At these wavelengths we also notice the presence of several

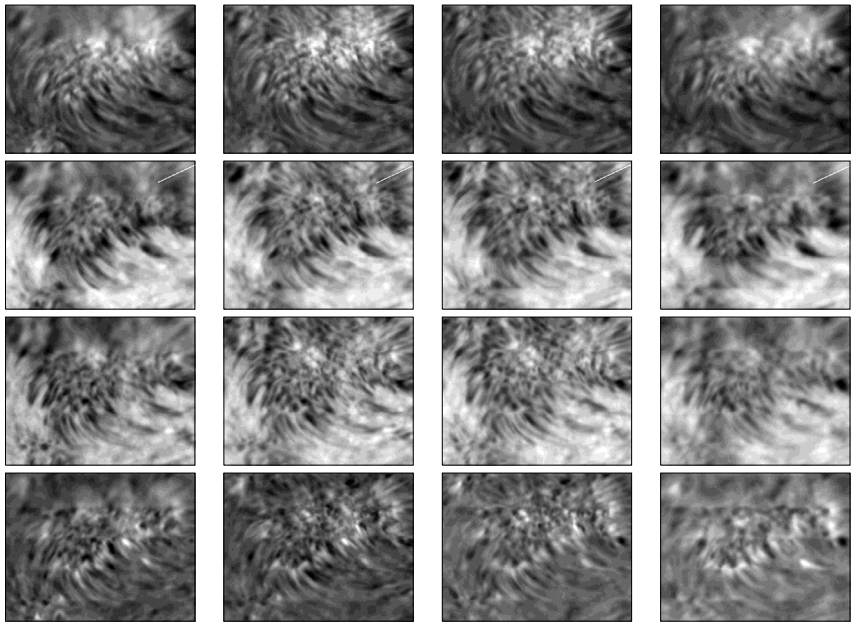

Fig. 2. A sequence of four intensity images (74″× 58″) at Hα line center (top row), at Hα+0.48 Å (second row) and at Hα–0.48 Å (third row) and the corresponding Doppler velocity images at H$\alpha\pm$0.48 Å (fourth row, bright corresponds to downflows) of the rosette of region A. The observations are from 10:15:36 to 10:17:41 UT with a cadence of about 40.5 s. The overplotted lines, which appear in the upper right corners of each of the four panels in the second row, correspond to the cut along the mottle used for the time slice images of Fig. 6a.

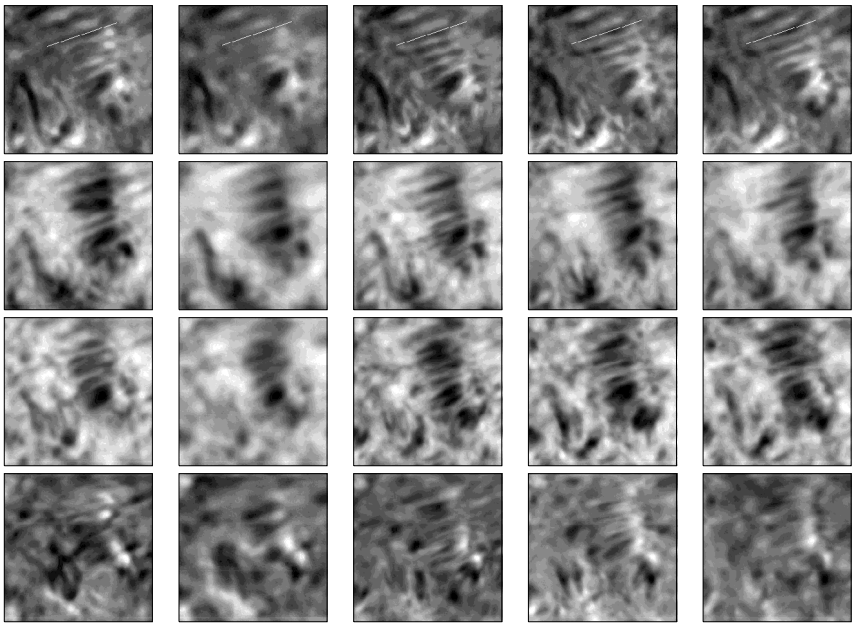

Fig. 3. A sequence of five intensity images (38″× 38″) at Hα line center (top row), at Hα+0.48 Å (second row) and at Hα–0.48 Å (third row) and the corresponding Doppler velocity images at H$\alpha\pm$0.48 Å (fourth row) for the mottles of region B. The observations are from 10:14:11 to 10:16:59 UT and the cadence is about 40.5 s. The overplotted lines, which appear in the upper part of each of the four panels in the first row, correspond to the cut along the mottle used for the time slice images of Fig. 6b.

small bright more or less circular structures inside the core of the rosette which are also visible but more diffuse at line center.

In Fig. 3 a time sequence of region B at Hα line center, Hα+0.48 Å, Hα–0.48 Å and the Doppler velocity at H$\alpha\pm$0.48 Å is shown. This region is located below the main body of the filament (see Fig. 1). It consists of eight to nine (depending on the frame) almost parallel elongated dark mottles, forming a chain and having their roots towards the body of the filament. Their inclination seems more horizontal than vertical to the solar surface, their typical thickness is ∼2″ and their length close to 15″. They stay mostly straight during our observations, slightly diverging and changing their direction in some frames. Sometimes nearby mottles seem to merge to form a unique structure or split in two, but this could be an artifact due to the spatial resolution and/or to the change of the seeing. Their shape and length, however, clearly change from frame to frame as it can clearly be seen in the time sequence of Fig. 3. Most of them can be followed for the whole duration of the 27 min time series used in this study. Bright structures, called "filigree" by Dunn & Zirker (1973), are visible at the footpoints of mottles, especially at Hα–0.48 Å, implying the presence of downflowing material. Bright mottles are clearly visible in the Hα line center image and are found in close

juxtaposition with dark mottles. Their visibility fades as one moves away from the Hα line center.

There is a third region of mottles (region C) in the middle of the left part of the image, to the left of the filament body. Only half of the region is found inside the field-of-view, but it seems that it has a rosette-like structure, much smaller than rosette A. Mottles of the upper half of the rosette are curved too (like those of region A) counter-clockwise affected by the magnetic field of the filament. The number of grains is suppressed in the core of this rosette.

2.2.2. Doppler velocity maps

The most apparent feature in the Doppler velocity map is the reduced velocity amplitude in the filament channel which crosses almost diagonally the image compared to the velocity of the surrounding region (Fig. 1, bottom panel). This could be due to the integrated effect of several threads found along the line-of-sight and having opposite velocities or to the existence of horizontal velocities which do not contribute very much to the measured line-of-sight Doppler velocities.

In the central part of the rosette of region A, Doppler velocities are seen and stay for the duration of our sequence mostly positive (downward velocities, see Fig. 2, fourth row). However, we also find a large number of small round-shaped patches of upward and downward velocities, which are probably related to the round-shaped dark and bright structures clearly seen in the intensity maps. The pattern of dark elongated structures, observed in the intensity maps, is also visible in the Doppler velocity maps. These dark velocity structures corresponding to upward velocities are clearly distinguishable from the local background and are well separated from each other. Their limits do not coincide with the limits of the dark mottles seen in the intensity maps of Figs. 2 and 3. The footpoints of mottles are red-shifted (downward velocities) most of the time, something clearly seen in the Hα–0.48 Å intensity maps and the Doppler velocity images of the chain of parallel mottles of region B, where individual mottles can be easily followed (Fig. 3, fourth row), but also from the chain of bright points at the footpoints of mottles of region A (Fig. 2). This implies that the well-known filigree which outline the supergranular cells and are especially prominent in the red wing of Hα could be the red-shifted footpoints of mottles. The behaviour, however, of the upper parts of the mottles is somewhat different. They appear first blue-shifted in some frames and then red-shifted and this velocity pattern seems to be repeated with time as it has already been noticed by Tsiropoula et al. (1994). We will further explore this particular behaviour of mottles below with a detailed velocity analysis.

2.2.3. MDI magnetograms

Magnetograms taken every one minute with the Michelson Doppler Imager (MDI) onboard *SOHO* are available for the whole duration of our observations. Unfortunately the Hα field-of-view is outside the high resolution box area of MDI so only low resolution magnetograms with a spatial resolution of $\sim 2''$ are available. In Fig. 4 we show the magnetogram of the observed area taken almost at the same time (10:16 UT) as the Hα image shown in Fig. 1. On the magnetogram the entire two-dimensional Hα intensity image is overplotted after taking into account information in the headers of the respective images and carefully aligning some features common to the magnetogram and the Hα image. We clearly see that the rosettes of region A and C extend well outside the observed Hα field-of-view. Region A is related to a region where strong magnetic fields up to a few hundred Gauss are observed. It is not certain whether dark and/or bright grains observed inside the rosette are related or not to the elongated mottles that outline the boundary of the central region of the rosette. However, it is interesting to notice the correlation of the inclination of these structures observed in region A with the longitudinal component of the magnetic field measured by MDI. In the core of the rosette, which coincides with an active region and a large strength of the longitudinal magnetic field, the features have a round shape indicating that they are almost vertical on the solar surface. Around the central region, the strength of the longitudinal magnetic field decreases and the mottles become more and more elongated as we go away from the core. This behaviour implies that features observed in the central region of the rosette are related to a strong vertical component of the magnetic field, while mottles are related to its horizontal component. Lites et al. (1996) reported the presence of weak (significantly less than 1000 G) horizontal magnetic fields, which tend to occur closer to the boundaries of the supergranular cells, typically lasting $\sim$5 min, although they were unable to find an association with chromospheric features. No clear magnetic pattern is associated with the mottles of region B, while an enhanced ring-shaped magnetic flux outlines the core of rosette C. The magnetogram is not sensitive enough

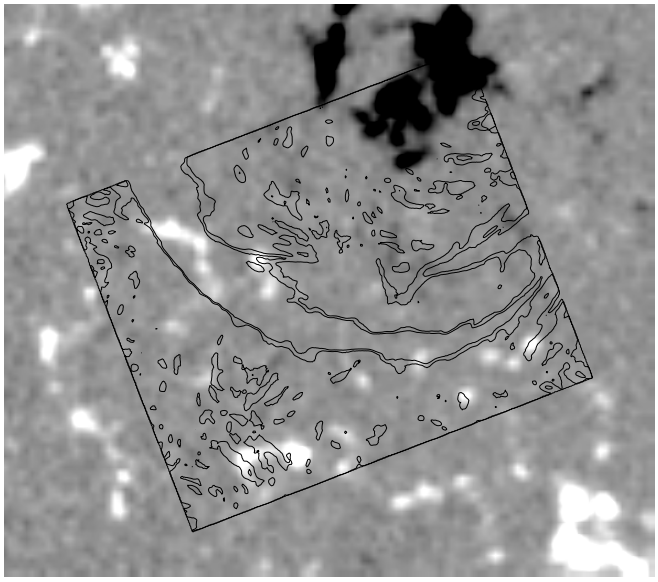

Fig. 4. Hα intensity contours of the entire field-of-view observed with THEMIS overplotted on an MDI magnetogram taken at almost the same time.

to permit us to clarify whether there is a mixed polarity flux distributed on a small scale inside the core or at the boundaries. The calculated noise σ is of the order of 8 Gauss and the magnetic field around the footpoints of the mottles is close to this value. Thus, observed small dynamic changes of the magnetic field cannot be considered as real. Moreover, the MDI spatial resolution of $\sim 2''$, which is of the order of the width of the observed mottles, does not permit us to correlate dynamic changes of mottles with changes of the magnetic field.

3. Computational procedure

Various methods have been used in the past for the deduction of different physical parameters of chromospheric structures from observations in the Hα line. The most widely applied technique is the so called "cloud" model, introduced by Beckers (1964). It considers the structure as a "cloud" lying between the observer and a uniform atmosphere described by a reference "background" profile which is assumed to be the same below the structure and in its surrounding atmosphere. Although the derivation of physical conditions in individual structures from observations needs – in principle – multi-dimensional solutions of the time-dependent non-LTE transfer equations, the "cloud" model provides a good representation of the observed profiles and a reliable quantitative description of the spatial distribution of the physical parameters responsible for the observed intensity inhomogeneities in the body of the structure (Alissandrakis et al. 1990; Tsiropoula et al. 1993). The cloud model works quite well for optically thin structures and considers for an observed profile $I(\Delta\lambda)$ the contrast profile

$$C(\Delta\lambda) = \frac{I(\Delta\lambda) - I_0(\Delta\lambda)}{I_0(\Delta\lambda)} = \left(\frac{S}{I_0(\Delta\lambda)} - 1\right)(1 - \mathrm{e}^{-\tau(\Delta\lambda)}) \quad (1)$$

with a Gaussian wavelength dependence for the optical thickness

$$\tau(\Delta\lambda) = \tau_0 \, \mathrm{e}^{-\left(\frac{\Delta\lambda - \Delta\lambda_\mathrm{I}}{\Delta\lambda_\mathrm{D}}\right)^2} \quad (2)$$

where $I_0(\Delta\lambda)$ is the reference profile emitted by the background and $\Delta\lambda_\mathrm{I} = \lambda_0 v/c$ is the Doppler shift with λ_0 being the line center wavelength and c the speed of light. The four adjustable parameters of the model are the source function S, the Doppler width $\Delta\lambda_\mathrm{D}$, the optical depth τ_0 and the line-of-sight velocity v. All these parameters are assumed to be constant through the structure.

For the calibration of the observed profiles relative to the quiet Sun continuum we have associated the line center counts of the flat field profile of our observations (which was taken close to the center of the Sun) with the line center quiet-Sun Hα intensity value of 0.169.

The background profile used in this analysis is taken as the mean of all profiles of a region around the mottles that have a line center intensity higher than the quiet-Sun value of 0.169. This way we simulate the fact that the background atmosphere of the structures under study is more active than the quiet Sun. The obtained line center intensity value of the background is $\sim$0.185 and depends on the image of the time series. An error in the background intensity leads to errors in the calculation of the source function S, the optical thickness τ_0 and the amplitude of the velocity v but not of the velocity sign (see Discussion).

In our analysis we process profiles that have a maximum value of contrast $C(|\Delta\lambda|) \leq 0.48$ Å) less than 0.05 instead of zero, in order to consider profiles with positive contrast due to instrumental noise and the fact that the background profile is not exactly known. We use an iterative least-square procedure for non-linear functions described in Alissandrakis et al. (1990) for the computation of the aforementioned four parameters that best describe an observed profile. As initial values for the iteration procedure we take a value of 1 for the optical depth τ_0 at line center, a Doppler width $\Delta\lambda_\mathrm{D}$ of 0.3 Å and a velocity v of zero. As for the initial value of the source function S we use the empirically-found approximate relation $S = 0.155 + 0.159 \times C(\Delta\lambda = 0)$. This iterative procedure is repeated until the difference between two consecutive χ^2 values is smaller than 0.01% and for a maximum number of 300 iterations. However, the iteration procedure usually converges after less than 20 iterations. After this fitting procedure, values of S greater than 0.19 were rejected because they correspond to optically thick structures for which the cloud model is not valid.

As we have already mentioned we have intensity values at five wavelengths in the Hα profile: at line center, at ± 0.24 Å and at ± 0.48 Å. However, these wavelengths are rather close to the core of the profile. For high velocities the lack of intensity values at wavelengths close to the wings of the profile can lead to an over/underestimation or even a wrong calculation of the Doppler width $\Delta\lambda_\mathrm{D}$ and line-of-sight velocity v. For this reason two more values have been used for the fitting procedure: the contrast at ± 1 Å from the line center (wings of the profile) was set equal to zero. This is based on the fact that past observations of the Hα profile of several chromospheric "cloud" structures show that at the wings of the profile ($\Delta\lambda \geq \pm 1$ Å) the observed intensity becomes almost equal to the background intensity as we approach the continuum. The influence of this assumption on the calculation of the physical parameters of the structures will be discussed in the next section.

4. Results

Below we present the results obtained from the application of the cloud model to the observed profiles of mottles of region B that have – as we have already mentioned – a maximum value of contrast C less than 0.05 and taking into account the conditions for its validity (Alissandrakis et al. 1990). We discuss the global properties of mottles as well as the time evolution of certain physical parameters along individual mottles.

4.1. Global properties of mottles

In Fig. 5 we show the histograms of velocity v, optical thickness τ_0, Doppler width $\Delta\lambda_\mathrm{D}$ and source function S derived from the cloud model applied for all the mottles of region B (eight to nine depending on the frame, see Fig. 1) for all forty images

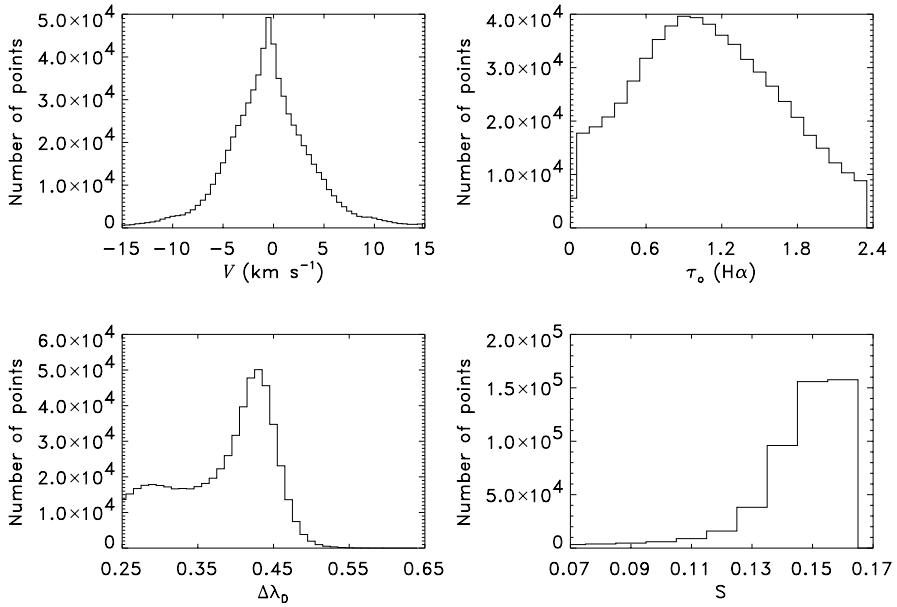

Fig. 5. Histograms of velocity v, optical thickness τ_0, Doppler width $\Delta\lambda_D$ and source function S derived from the cloud model for the mottles of region B.

of the time series. The velocity distribution, which varies between -15 and 15 $\mathrm{km\,s^{-1}}$, is almost symmetric, indicating the presence of both downflows and upflows and has a mean value of -0.1 $\mathrm{km\,s^{-1}}$ (upward velocity). The structures are mostly optically thin with an optical thickness distribution that peaks around 0.9. This is well reflected on the source function distribution which peaks close to 0.156, since optically thin structures allow more of the background radiation to be transmitted through them. The Doppler width distribution shows a peak around 0.43 Å and has a mean value of 0.35 Å. The rapid decrease of the distribution after 0.45 Å is a computational artifact due to the lack of observed intensities for $|\Delta\lambda| \geq 0.48$ Å and the assumed contrast of zero at $\Delta\lambda = \pm 1$ Å. Although this assumption leads always to a convergence for our iterative method, it results in an underestimation of the Doppler width for high velocities, since there are not enough points in the aforementioned wavelength range for the optimal fitting with the least square procedure. Assuming a microturbulence velocity of 15 $\mathrm{km\,s^{-1}}$, which is considered typical for such structures, we obtain from the mean value of the Doppler width a temperature of 11 000 K, which is in accordance with the temperatures inferred for chromospheric mottles.

4.2. Temporal evolution of physical parameters of individual dark mottles and dark grains

Time series of images offer a unique opportunity for the study of the spatial and temporal evolution of individual structures. Usually to follow individual mottles is not an easy task, since they change continuously, sometimes overlap with others and/or have curved trajectories. In Fig. 6 we present the distribution of physical parameters along the central axes of two individual mottles, indicated by the white lines in Figs. 2 and 3, as a function of time (time slice images). These mottles are straight and well separated from the others. To obtain the time slice images we averaged the respective physical parameters over a strip extending 0.3″ on either side of the main axes of the mottles which are carefully traced, taking into account a good superposition as well as small changes in direction on each image of our time sequence. These parameters are: the optical thickness τ_0 (top row), the source function S (middle row), and the velocity v (bottom row). The left side of all images corresponds to the feet of the mottles. We see that the body of the mottles under consideration remains mostly optically thin with an optical thickness around one. The source function is of the order of 0.14, with the higher values occurring close to the feet of the mottles where the structures emerge from the solar surface. On the velocity time slice images we have overplotted some contours of downward (positive) and upward (negative) velocities, as well as the contour of zero velocity. On the velocity images it is clearly seen that the material is almost always descending near the footpoints of the mottles. Higher up there are moments when all (or mostly all) of the material is moving downwards towards the footpoints of the structures. As time progresses, the velocity behaviour usually changes to one where material in the lower part of the mottles is falling down towards the feet of the structures while the material in the upper part is moving upwards. As one would expect from a violent upward motion of the plasma, these upward velocities are often associated with an increase of the optical thickness of the structure and a small enhancement of the source function. This recurrent pattern of downward motion followed by both upward and downward motions seems to have a timescale of ∼5 min. This behaviour is encountered not only at these two mottles presented here but in several other mottles of the considered areas.

The quasi-periodic behaviour of the velocity is also apparent in the dark grains found in the core of the rosette of region A. Since the cloud model is not applicable in structures standing vertically on the solar surface we use Doppler velocities to examine the behaviour of flows in the dark grains. However, we must point out that cloud velocities obtained

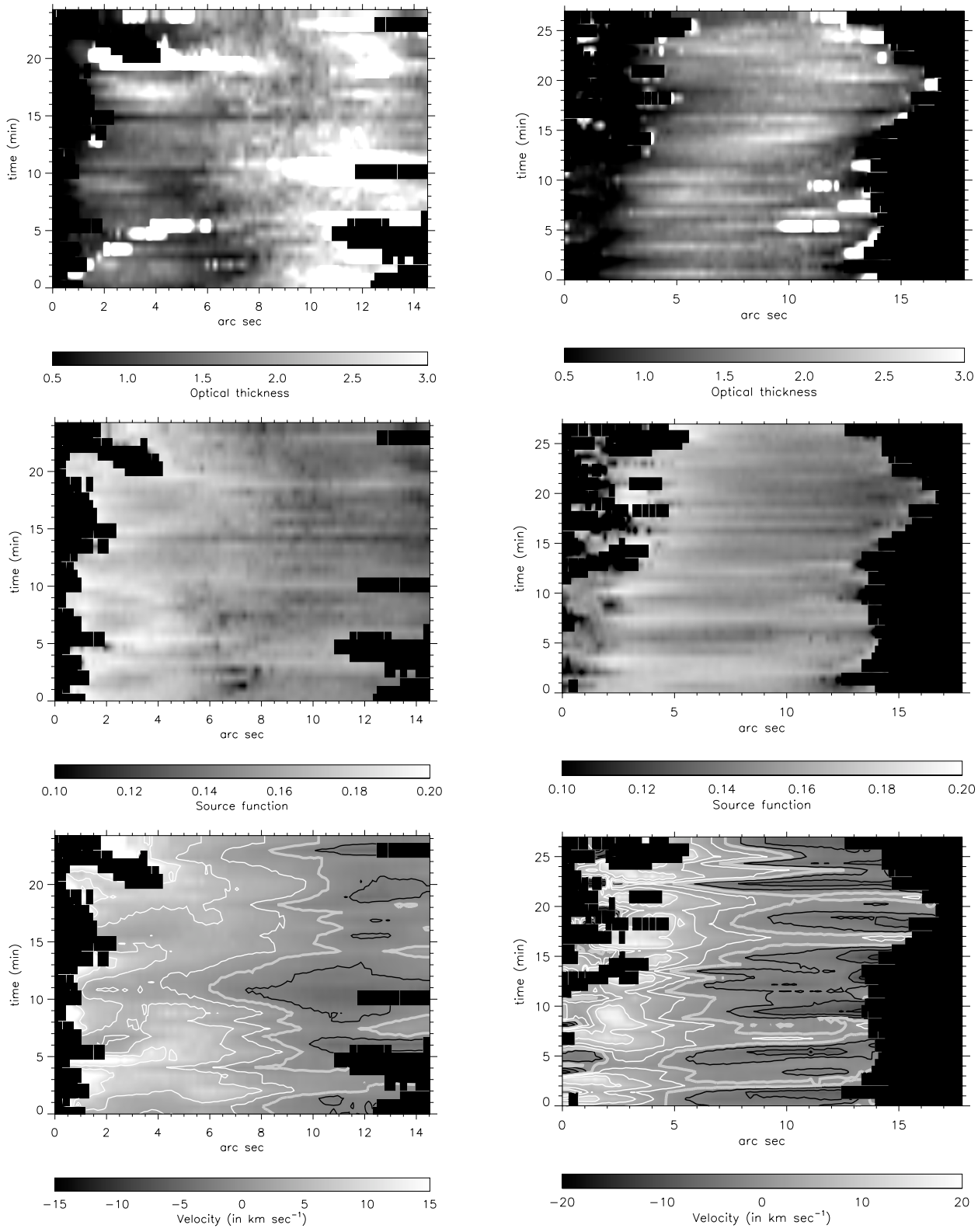

Fig. 6. Time slice images of optical thickness $\tau_{\max}$ (top row), source function S (middle row) and velocity v (bottom row) for a cut through a mottle of **a)** region A (left column) and **b)** region B (right column). The mottles are indicated with white lines in Figs. 2 and 3 respectively. On the velocity images, the black contours denote upward velocities, the white contours downward velocities while the thick gray line represents the zero velocity contour.

from non-LTE models are higher, usually by a factor of two, than Doppler velocities (Alissandrakis et al. 1990). In Fig. 7 we show the average Doppler velocity at ±0.48 Å as a function of time for two different dark grains inside this rosette.

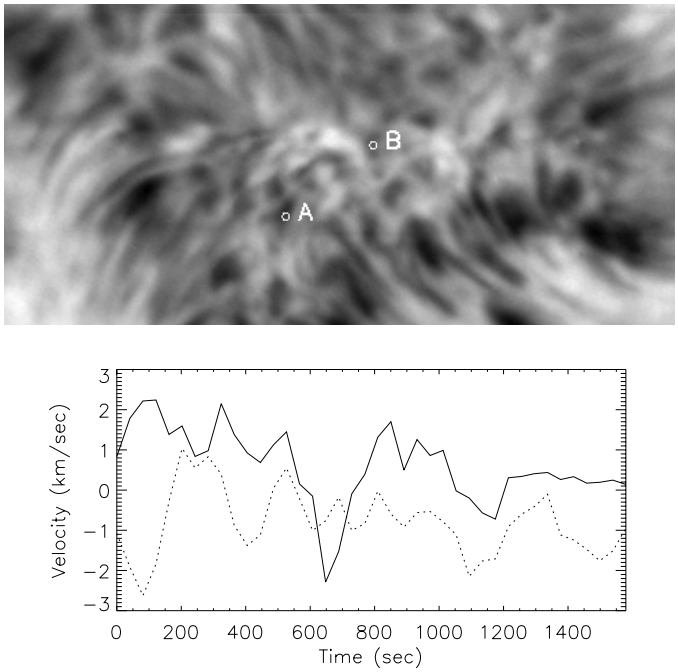

Fig. 7. Top: a part of region A showing the two dark grains (marked as A and B) under study. Bottom: the observed average Doppler velocity variations (see text) at ±0.48 Å for the two chromospheric dark grains (solid line corresponds to dark grain A and dotted line to dark grain B).

This average Doppler velocity is calculated within a 5 × 5 pixels square around the center of the grain which was carefully traced in all images of the time sequence. As can be seen in Fig. 7, Doppler velocities change with time showing a quasi-periodic behaviour of ∼5 min, as cloud velocities show in mottles. Apart from the similarity of the quasi-periodic behaviour of the Doppler velocities the upward and downward behaviour of the flows observed in grains could also be considered as similar to that of flows observed in mottles; e.g., bi-directional flows followed by downflows. The observed Doppler velocities represent the net velocity component along the line-of-sight. A bi-directional flow along a structure vertical to the solar surface will have as a result a positive or negative velocity of small amplitude depending on the magnitudes of the opposite velocities. Based on these two similarities, we speculate that dark grains are structures similar to mottles, their difference being their inclination relative to the solar surface.

Both the quasi-periodic behaviour of velocity in dark mottles and of Doppler velocities in dark grains implies some kind of periodicity, with periods of the order of ∼5 min. However, no definite answer can be given without a detailed power spectrum analysis. A wavelet spectral analysis of the temporal behaviour of velocities and intensities in dark mottles and grains is currently under way and the results will be reported in a forthcoming paper.

4.3. Outline of a mechanism explaining the dynamical behaviour of mottles and grains

Figure 6 clearly indicates a bi-directional behaviour of the velocity as a function of time and space in two mottles found in two different regions, region A (Fig. 2) and region B (Fig. 3), with downflows at their footpoints and upflows at their tops. This bi-directional flow is followed by downflowing material along the whole structure. That is, the upper parts of the mottles show flows in both directions while the bottom parts show flows in the downward direction only and the whole process is repeated with a period of ∼5 min. We remind the reader that such a behaviour has already been noticed in Hα Doppler and cloud velocity variations of mottles observed near the solar disc center by Tsiropoula et al. (1994). Two kinds of motions should be considered as responsible for these flow patterns: a) one similar to that of a jet where material is ejected upwards and subsequently, due to gravity, material at the lower part of the jet is falling towards the footpoints, while the upper part is still rising; then material is falling along the whole structure and b) magnetic reconnection, which would drive material out of the reconnection region in opposite directions. In case (a) we should be able to observe high upwards velocities related to the ejection of the jet. However, no such velocities are observed. This fact leads us to suggest that mottles are closely related to the magnetic flux cancellation process and that magnetic reconnection is the responsible mechanism for the formation and dynamics of these structures. The study of the intensity and Doppler velocity time sequence also indicates – as we have previously mentioned – that individual mottles appear in bursts, they last typically for about 5 min and usually reappear several times in the same location.

Mottles are mostly found at the network boundaries, while grains are found inside the cells. It is nowadays well established that at the photospheric level each cell is characterized by a horizontal flow of 0.3–0.4 km s^{-1} directed from its center towards the boundaries. Inside the cells small-scale magnetic fluxes of mixed polarity emerge continually and are swept by the supergranular flows to the cell boundaries, where mixed polarity flux elements are driven together by the photospheric flows. Magnetic fields either merge with fields of the same polarity or cancel with fields of opposite polarity (Wang et al. 1996; Schrijver et al. 1997) and this can occur not only at the boundaries, but also inside the cells. Therefore, the existence, geometry and dynamical behaviour of mottles and grains may be closely associated with this recycling of the magnetic field.

The observed velocity behaviour could be explained in the context of a simple reconnection model proposed by Pikel'ner (1969). A schematic representation of this model is given in Fig. 8 (of course, unipolar as well as bipolar fields of appropriate polarity could be involved, see Fig. 8 of Wilhelm 2000). According to this model, the squeezing of opposite polarity field lines at the chromospheric level leads to cooling by radiation of the compressed gas, which is trapped between them and consequently to a downflow due to gravity (left part of Fig. 8). When opposite field lines come too close and reconnection occurs then part of the material is carried upward by the reconnected field lines, while the material below the reconnection region moves downwards under the action of both gravity and magnetic forces (middle and right part of Fig. 8). This cycle is repeated until the field is annihilated. Analyzing the same set of data, Tziotziou & Tsiropoula (2002) have shown that sometimes there is a temperature excess at the location where

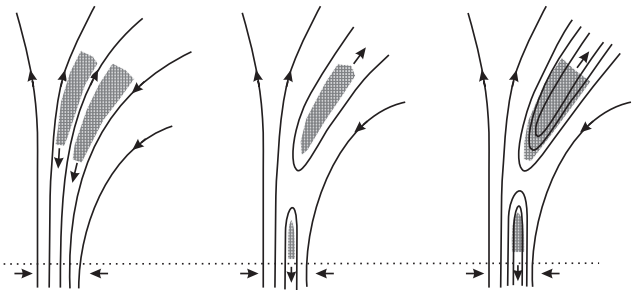

Fig. 8. A simple reconnection model (see text) explaining the observed velocity behaviour in mottles.

reconnection occurs, indicating the presence of local heating. However the amount of the released magnetic energy which is converted to heating needs to be further explored.

5. Discussion and conclusions

A long time series of high-spatial and temporal resolution observations of chromospheric fine structures in a 2-D field-of-view has been analyzed. The results highlight the importance of two-dimensional observations, like the ones provided by the MSDP spectrograph, for the study of the dynamical behaviour of evolving solar structures. Several physical parameters describing chromospheric dark mottles have been obtained by means of the cloud model. The cloud model allows a fast and reliable extraction of information concerning the most important physical parameters describing cloud-like structures, like mottles, fibrils, arch filaments, etc. However, it should be pointed out that the reliability of the determination of the various physical parameters using this model depends on various factors. One of them is the right choice of the background intensity that illuminates the structure. This is, because the background influences: a) the convergence of the method to a valid solution and b) the calculation of the optical depth associated with the structure, since it is the most sensitive parameter to the observed contrast. The estimation of the background is usually based on the visual inspection of the surrounding atmosphere, i.e. whether the structure is standing above a quiet solar surface or a more active region like a rosette. Furthermore, for non-LTE models, where the source function is not constant but is defined by the radiation field in the structure as a function of optical depth (Mein et al. 1996; Heinzel et al. 1999), the source function does not depend much on the velocity of the structure. On the contrary, under the constant source function assumption, it strongly depends on the velocity especially for very small optical depths. As a consequence, since velocity is well defined by the cloud model, the source function affects the correct computation of the optical thickness in the case of high velocities. It is obvious that more precise non-LTE calculations, with a variable source function defined by the radiation field inside the structure are needed for a precise determination of both the source function and optical thickness that best describe the structure (see Molowny-Horas et al. 1999; Tziotziou et al. 2001). Another point to be made is that application of the cloud model to structures that exhibit high upward and/or downward velocities reveals the necessity of obtaining Hα profiles that extend well into the wings of the line. In the absence of such profiles, convergence to a solution is not reliable or even possible for high velocities, since Doppler shifts are in this case significant.

After pointing out the limitations of the application of the cloud model we argue that it is still an extremely reliable method for the study of optically thin structures in absorption, like dark mottles. Heinzel & Schmieder (1994), using non-LTE models, have concluded that for low pressure structures (<0.5 dyn/cm^2), as it is the case for dark mottles, the cloud model can be applied and gives reliable results. Furthermore, in this analysis we are mostly interested in velocity distributions within dark mottles. As shown by Alissandrakis et al. (1990) the velocity is the least model-dependent parameter and thus the obtained velocity values provide a good qualitative and, most times, a reliable quantitative representation of the actual velocity.

The spatial distribution of dark mottles and grains as well as the temporal behaviour of respectively their cloud and Doppler velocities leads us to suggest the similarity of both structures. Both structures show a quasi-periodic behaviour of $\sim$5 min and the net Doppler velocity amplitude in grains, taking into account the ratio inferred by previous calculations of – at least – two between the cloud and Doppler velocities, seems to be of the right order. Flows along mottles are clearly bi-directional, while flows in grains could also be bi-directional, although no definite proof cannot be provided since they are almost parallel to the line-of-sight. Their different appearance seems to be related to their inclination, with mottles more horizontal to the solar surface and grains almost vertical to it. Unfortunately, application of the cloud model is not possible in the case of grains in order to test the similarity of other parameters. Since they are structures vertical to the surface and of finite cross-section, they cannot be considered as "clouds" illuminated from below by a uniform background. Recently, round-shaped structures found at the boundaries and inside the cells of the network were studied by Lee et al. (2000) and Chae et al. (1998a, 1998a). They called these events upflow events and distinguished them into two types, type I (broad and blueshifted compared to the quiet sun profile) and type II (broad and blueshifted, but displaying also an emission in the red wing). The latter were identified as corresponding to dark grains. A study of several upflow events with a cloud model and a comparison of the obtained parameters with those of dark mottles lead them to the conclusion that they are not associated with dark mottles. However, since the cloud model cannot be applied to these structures, they attribute to them values which are not correct. We suggest that the round-shaped structures they call "upflow events" are essentially the same as the dark mottles, the only difference being the respective inclinations relative to the solar surface and the line-of-sight with Earth. Of course, this idea must be tested further.

Over the past years, high-resolution observations of photospheric, chromospheric and transition region networks have improved substantially in quality. Apart from the well-known dark and bright mottles, spicules and dark grains, many

complicated and dynamic fine structures have been discovered in association with the network boundaries and cells, like explosive events, network flares, upflow events, Hα–1 Å jets. However, their interpretation and interrelationship remains ambiguous, because the same feature has a different appearance when observed in different spectral lines. The common picture for all these events that comes out from analyses of observational data is that they are all related to the continually changing magnetic fields of the low atmosphere. Thus, it is not surprising that most of them appear within the network, since many new bipolar elements emerge in the cells and drift to the boundaries by the supergranular flow. Interaction of the magnetic fields have as a result the enhancement of the flux concentration in the case of same polarities or its cancellation in the case of opposite polarities. Observations support the idea that flux cancellation is most likely the result of magnetic reconnection during which a bi-directional flow is emanating from the reconnection site. For most of the events mentioned above, magnetic reconnection has been suggested as the driving mechanism (see, e.g., Innes et al. 1997; Chae et al. 1998a; Wilhelm 2000).

In the present work the cloud and Doppler velocities obtained for dark mottles and grains found at the supergranular boundaries and cells respectively clearly show a bi-directional and recurrent character. Thus, it is reasonable to propose that magnetic reconnection is the driving mechanism for both structures. The choice of magnetic reconnection is supported by a) the bipolar nature of this process, which would drive material out of the reconnection region in opposite directions exactly as observations indicate in the case of mottles and could also happen in the case of grains and b) by the fact that these structures occur at the network boundaries and inside the network cells, where a continuous emergence and cancellation of the magnetic field is taking place. It seems that both structures are related to the fine structure of the magnetic field. However, the low resolution of the magnetograms provided by MDI does not allow the detailed study of the relationship between the small scale magnetic fields and the observed structures. High spatial and temporal resolution observations of the magnetic field vector are needed in order to follow the cancellation of bipolar magnetic elements and its identification as the source of mottles and grains.

Another interesting finding of our studies is that downflows along the whole mottle follow the observed bi-directional flows. Several observations of average redshifted EUV emission lines have indicated the presence of downflows in the transition region above the chromospheric network. This has led to the suggestion that the redshifts are caused by downward flowing spicular material that has cooled from coronal temperatures (Pneumann & Kopp 1978) or transition region temperatures (Withbroe 1983) falling back to the chromosphere. Our results could offer the observational evidence to support these suggestions. However, as there is no direct evidence that spicules are heated to the transition region or coronal temperatures, these suggestions must be verified by simultaneous observations of mottles/spicules obtained in chromospheric, transition region and coronal lines. On the other hand, downflows are always present at the footpoints of mottles. We claim that these downflows are related to the well-known "filigree" best observed in the red wing of Hα.

Our current understanding of the behaviour of the magnetic field in the quiet solar low atmosphere is that of the continual recycling of the magnetic flux through its emergence, transport, and cancellation related mainly to the network. In parallel, a "zoo" of fine-scale, transient structures have been observed in the chromosphere, transition region and low corona network. Although these structures seem to have different properties, they all appear to be related to small-scale magnetic reconnection. In this context, the comprehension of the dynamical behaviour of chromospheric dark mottles and its association with the magnetic field is crucial to understand the chromospheric dynamics, their possible relation to other structures and their contribution to the mass balance and heating of the overlying solar atmosphere.

Acknowledgements. The THEMIS telescope is operated on the island of Tenerife by CNRS-CNR in the Spanish Observatorio del Teide of the Instituto de Astrofísica de Canarias. We would like to thank S. Regnier (PI of the project) and C. Briand (observer) for providing the observations and the referee for comments and suggestions on improving the paper. We are also indebted to A. Anastasiadis and N. Mein for useful discussions and comments. This research is part of "Programme d'Actions Intégrées Franco-helleniques PLATON".

References

Alissandrakis, C. E., Tsiropoula, G., & Mein, P. 1990, A&A, 230, 200
Beckers, J. M. 1963, ApJ, 138, 648
Beckers, J. M. 1964, A study of the fine structures in the solar chromosphere, Ph.D. Thesis, Utrecht
Beckers, J. M. 1968, Sol. Phys., 3, 367
Beckers, J. M. 1972, ARA&A, 10, 73
Bray, R. J., & Loughhead, R. E. 1974, The Solar Chromosphere (London: Chapman and Hall)
Chae, J., Wang, H., Lee, C.-Y., Goode, P. R., & Schühle, U. 1998a, ApJ, 497, L109
Chae, J., Wang, H., Lee, C.-Y., Goode, P. R., & Schühle, U. 1998b, ApJ, 504, L123
Dara-Papamargaritis, H., & Koutchmy, S. 1983, A&A, 125, 280
Dunn, R. B., & Zirker, J. B. 1973, Sol. Phys., 33, 281
Elliott, I. 1969, Sol. Phys., 6, 28
Heinzel, P., & Schmieder, B. 1994, A&A, 282, 939
Heinzel, P., Mein, N., & Mein, P. 1999, A&A, 346, 322
Innes, D. E., Inhester, B., Axford, W. I., & Wilhelm, K. 1997, Nature, 386, 811
Lee, C.-Y., Chae, J., & Wang, H. 2000, ApJ, 545, 1124
Lippincott, S. L. 1957, Smiths. Contr. Astrophys., 2, 15
Lites, B. W., Leka, K. D., Skumanich, A., Martínez Pillet, V., & Shimizu, T. 1996, ApJ, 460, 1019
Mein, N., Mein, P., Heinzel, P., et al. 1996, A&A, 309, 275
Mein, P. 1991, A&A, 248, 669
Mein, P. 2002, A&A, 381, 271
Molowny-Horas, R., Heinzel, P., Mein, P., & Mein, N. 1999, A&A, 345, 618

Mouradian, Z. 1965, Ann. Astrophys., 28, 805
Pasachoff, J. M., Noyes, R. W., & Beckers, J. M. 1968, Sol. Phys., 5, 131
Pikel'ner, S. B. 1969, Astron. Zh., 46, 328
Pneumann, G. W., & Kopp, R. A. 1978, Sol. Phys., 57, 49
Rutten, R. J. 1999, in 3rd Advances in Solar Physics Euroconference: Magnetic Fields and Oscillations, ed. B. Schmieder, A. Hofmann, & J. Staude, ASP Conf. Ser., 184, 181
Schrijver, C. J., Title, A. M., Van Ballegooijen, A. A., Hagenaar, H. J., & Shine, R. A. 1997, ApJ, 487, 424
Solanki, S. K. 1993, Space Sci. Rev., 63, 1
Sterling, A. C. 2000, Sol. Phys., 196, 79
Suematsu, Y., Wang, H., & Zirin, H. 1995, ApJ, 450, 411
Tsiropoula, G., Alissandrakis, C. E., & Schmieder, B. 1993, A&A, 271, 574
Tsiropoula, G., Alissandrakis, C. E., & Schmieder, B. 1994, A&A, 290, 285
Tsiropoula, G., & Schmieder, B. 1997, A&A, 324, 1183
Tziotziou, K., Heinzel, P., Mein, P., & Mein, N. 2001, A&A, 366, 686
Tziotziou, K., & Tsiropoula, G. 2002, Proc. 10th. European Solar Physics Meet., Solar variability: From core to outer frontiers, ESA SP-506, 787
Uchida, Y. 1969, Publ. Astron. Soc. Japan, 21, 128
Wang, H., Tang, F., Zirin, H., & Wang, J. 1996, Sol. Phys., 165, 223
Wilhelm, K. 2000, A&A, 360, 351
Withbroe, G. L. 1983, ApJ, 267, 825